



Chinese Pharmaceutical Association
Institute of Materia Medica, Chinese Academy of Medical Sciences

Acta Pharmaceutica Sinica B

www.elsevier.com/locate/apsb
www.sciencedirect.com



ORIGINAL ARTICLE

Development of the novel ACLY inhibitor 326E as a promising treatment for hypercholesterolemia



Zhifu Xie^{a,†}, Mei Zhang^{a,†}, Qian Song^{a,b,†}, Long Cheng^{a,b},
Xinwen Zhang^a, Gaolei Song^{a,b}, Xinyu Sun^a, Min Gu^a,
Chendong Zhou^a, Yangming Zhang^{a,c}, Kexin Zhu^a, Jianpeng Yin^d,
Xiaoyan Chen^a, Jingya Li^{a,b,*}, Fajun Nan^{a,b,d,*}

^aState Key Laboratory of Drug Research, Shanghai Institute of Materia Medica, Chinese Academy of Sciences, Shanghai 201203, China

^bUniversity of Chinese Academy of Sciences, Beijing 100049, China

^cBurgeon Therapeutics Co., Ltd., Shanghai 201203, China

^dDrug Discovery Shandong Laboratory, Bohai Rim Advanced Research Institute for Drug Discovery, Yantai 264117, China

Received 21 February 2022; received in revised form 24 April 2022; accepted 30 May 2022

KEY WORDS

Hypercholesterolemia;
Atherosclerosis;
Liver;
ATP-Citrate lyase
(ACLY);
Lipogenesis;
Cholesterol efflux;
ACLY inhibitor

Abstract Hepatic cholesterol accumulation is an important contributor to hypercholesterolemia, which results in atherosclerosis and cardiovascular disease (CVD). ATP-citrate lyase (ACLY) is a key lipogenic enzyme that converts cytosolic citrate derived from tricarboxylic acid cycle (TCA cycle) to acetyl-CoA in the cytoplasm. Therefore, ACLY represents a link between mitochondria oxidative phosphorylation and cytosolic *de novo* lipogenesis. In this study, we developed the small molecule **326E** with an enedioic acid structural moiety as a novel ACLY inhibitor, and its CoA-conjugated form **326E**-CoA inhibited ACLY activity with an $IC_{50} = 5.31 \pm 1.2 \mu\text{mol/L}$ *in vitro*. **326E** treatment reduced *de novo* lipogenesis, and increased cholesterol efflux *in vitro* and *in vivo*. **326E** was rapidly absorbed after oral administration, exhibited a higher blood exposure than that of the approved ACLY inhibitor bempedoic acid (BA) used for hypercholesterolemia. Chronic **326E** treatment in hamsters and rhesus monkeys resulted in remarkable improvement of hyperlipidemia. Once daily oral administration of **326E** for 24 weeks prevented the occurrence of atherosclerosis in ApoE^{-/-} mice to a greater extent than that of BA treatment. Taken together, our data suggest that inhibition of ACLY by **326E** represents a promising strategy for the treatment of hypercholesterolemia.

*Corresponding authors.

E-mail addresses: jyli@simmm.ac.cn (Jingya Li), fjnan@simmm.ac.cn (Fajun Nan).

†These authors made equal contributions to this work.

Peer review under responsibility of Chinese Pharmaceutical Association and Institute of Materia Medica, Chinese Academy of Medical Sciences.

<https://doi.org/10.1016/j.apsb.2022.06.011>

2211-3835 © 2023 Chinese Pharmaceutical Association and Institute of Materia Medica, Chinese Academy of Medical Sciences. Production and hosting by Elsevier B.V. This is an open access article under the CC BY-NC-ND license (<http://creativecommons.org/licenses/by-nc-nd/4.0/>).

1. Introduction

Hypercholesterolemia, defined as excessive plasma cholesterol and low-density lipoprotein cholesterol (LDL-C) levels, is increasing globally prevalent. It has been estimated that over a third of the adult population develops hypercholesterolemia, which has become the lead causes of cardiovascular disease (CVD) worldwide^{1,2}. Thus, effective treatment of hypercholesterolemia has become a public health burden.

The current clinical therapeutic strategy to lower LDL-C is an effective method to control the progression of CVD and atherosclerotic cardiovascular disease (ASCVD)³⁻⁶. Statins inhibit 3-hydroxy-3-methyl-glutaryl-CoA reductase (HMGCR), the rate-limiting enzyme of hepatic cholesterol synthesis, leading to decrease LDL-C concentrations in hypercholesterolemia patients. The general effectiveness of statins, both in reducing LDL-C levels and decreasing CVD associated complicating disease has led to increasing access to these drugs by patients⁷⁻⁹. However, many at-risk patients do not achieve sufficient LDL-C lowering effects or are intolerant to statins due to liver- or muscle-related side effects^{10,11}. Furthermore, statin intolerance may lead to a 50% increase in recurrent myocardial infarction or coronary heart disease events compared to those with no statin use^{12,13}. Proprotein convertase subtilisin/kexin type 9 (PCSK9) inhibition lowers LDL-C by reducing the degradation of low-density lipoprotein receptor (LDLR) in hepatocytes^{14,15}. Recently, PCSK9 inhibitors (monoclonal antibodies and small interfering RNA) have emerged as an effective lipid-lowering therapy. However, current PCSK9 inhibitors need to be administered by injection and are costly, which may restrict their clinical use¹⁶⁻¹⁸. For these reasons, there is great interest in identifying novel LDL-C lowering therapeutics associated with a lower percentage of residual side effects that have convenient for administration for hypercholesterolemia treatment^{19,20}.

De novo lipogenesis in the liver is physiologically initiated by dietary carbohydrate intake and promotes energy storage through the insulin receptor substrate (IRS)-AKT signaling axis. Cytosolic acetyl-CoA serves as common substrate for fatty acids and cholesterol synthesis²¹⁻²³. Briefly, synthetic citrate from TCA cycle in the mitochondria is transported to the cytoplasm through tricarboxylate transport protein (SLC25a1). Cytoplasmic citrate is then rapidly cleaved by ACLY into acetyl-CoA and oxaloacetate^{24,25}. Acetyl-CoA is subsequently further converted to malonyl-CoA or mevalonate, from which fatty acids or cholesterol are subsequently synthesized^{21,22}. Besides, the elongation of very long chain fatty acids needs additional acetate supplied from gut microbiota or liver production²⁶. As previously study indicated that phosphorylation at Ser455 by AKT increases ACLY activity²⁷. Meanwhile, acetylation of ACLY at Lys540, Lys546, and Lys554 (ACLY-3K) by antagonizes its ubiquitylation and increases ACLY protein stability^{28,29}. Additionally, ACLY inhibition increases ATP binding cassette subfamily G member 5/8 (*Abcg5/8*) gene expression and is tightly correlated with hepatic cholesterol efflux into the intestine, which may also contribute to its modulation of cholesterol metabolism^{30,31}.

Dysregulation of hepatic ACLY activity or protein expression are connected to hepatic steatosis, type 2 diabetes (T2D) and hyperlipidemia³²⁻³⁵. Given its key role in hepatic lipid

metabolism, ACLY has been considered an attractive target for metabolic syndrome and lipid-lowering treatment³⁶. Despite widespread interest, few ACLY inhibitors have been described to date. Early discovery strategies have primarily focused on synthesizing citrate analogues³⁷. However, most of these candidates did not advance to clinical trials largely due to the insufficient cellular permeability and poor bioavailability. Bempedoic acid (BA, ETC-1002), a prodrug inhibitor of ACLY, has been recently approved by US Food and Drug Administration (FDA) as an additional therapeutic option in high-risk hypercholesterolemia patients who are unable to meet the goals using standard therapy³⁸⁻⁴⁰. Previous studies identified that BA was coupled into the active form BA-CoA responsible for ACLY inhibition by the very long-chain acyl-CoA synthetase-1 (ACSVL1), which is expressed primarily in the liver. The inactive conversion system for the prodrug in muscle explains the lack of myotoxicity⁴¹⁻⁴³. However, the clinical LDL-C lowering effect induced by BA with maximally tolerated statin therapy treatment was moderated (16.5% placebo-adjusted decrease from baseline at 12 weeks in LDL-C)³⁹.

In this study, we report the identification of a small molecule, **326E**, with an enedioic acid structural moiety as a novel ACLY inhibitor and demonstrate its potential therapeutic benefit in hypercholesterolemia. Our results show that ACLY inhibition by **326E** effectively improves hyperlipidemia in rodent and primate preclinical models, and intriguingly ameliorates the major hallmarks of atherosclerosis in ApoE^{-/-} mice by reducing hepatic lipogenesis and increasing cholesterol efflux into the intestine.

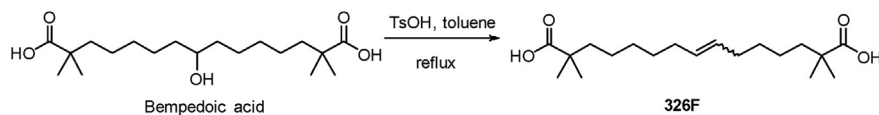
2. Results

2.1. Synthesis of **326F**

Bempedoic acid (BA), a prodrug of the ACLY inhibitor, is approved by FDA for hypercholesterolemia treatment and exerts a modest effect on LDL-C. Among our efforts to explore a more active ACLY inhibitor, we identified a simple dehydrated product of BA in the presence of *p*-toluenesulfonic acid (TsOH) in toluene and called it **326F** as shown in Scheme 1.

2.2. **326F** is more effective than BA on acetyl-CoA derived lipogenesis and gluconeogenesis

ACLY inhibition reduces lipogenesis in hepatocytes. To evaluate the effects of **326F**-induced ACLY inhibition on *de novo* lipogenesis, we treated mouse primary hepatocytes with **326F** for 24 h, and the incorporation rates of [1,2-¹⁴C]-acetate into fatty acids and cholesterol were determined. Our results showed a promising dose-dependent lipogenesis inhibition in response to **326F** treatment, which was more effective than BA treatment (Fig. 1A and B). Oxaloacetate, a carboxylic acid converted from citrate by ACLY, is the key substrate of hepatic gluconeogenesis. We determined that compared to BA treatment, the cumulative glucose production in primary hepatocytes was reduced with a greater tendency after **326F** intervention (Fig. 1C). Glutamine- α -ketoglutarate (α -KG) metabolism fuels the tricarboxylic acid cycle and attenuates the

Scheme 1 Synthesis of **326F**.

oxaloacetate deficiency induced by ACLY inhibition. Our results indicated that additional glutamine supplementation attenuated the inhibition of gluconeogenesis by **326F** and BA treatment (Fig. 1D). These data indicate that **326F**, a novel potential ACLY inhibitor, reduces *de novo* lipogenesis and gluconeogenesis to a greater extent than BA mouse primary hepatocytes.

2.3. Isomer **326E** but not **326Z** improves hyperlipidemia in a rodent model challenged by a HFHC diet

Considering that **326F** is a mixture with the proportion mix of conformations *E* and *Z*, we synthesized these two isomers, named **326E** and **326Z**, respectively, as shown in Scheme 2 (Fig. 1E). Compounds **1** and **2** were protected by 3,4-dihydro-2*H*-pyran (DHP) respectively, then coupling of alkynyl compound **3** and bromide **4** afforded compound **5**, which was then deprotected and bromination using an Appel reaction to give dibromide **6**. Alkylation of ethyl isobutyrate with **6** gave ester **7**. The subsequent hydrogenation of the alkyne in the presence of nickel acetate and sodium borohydride in ethanol led to the corresponding *cis*-alkene **8**, which was hydrolyzed to obtain **326Z**. Compound **5** was reduced with LiAlH₄ to obtain *trans*-alkene **9**, then **326E** was obtained using similar procedure as for **326Z**.

To probe cellular ACLY inhibition, we further investigated the lipogenesis inhibition effect of **326E** and **326Z** *in vitro*. Consistent with the **326F**, treatment with the new isomers **326E** and **326Z** reduced [1,2-¹⁴C]-acetate incorporated into fatty acids and cholesterol in a dose dependent manner and was more effective than BA treatment (Fig. 1F and G).

Hepatic ACLY inhibition reduces hepatic lipogenesis and improves dyslipidemia. To investigate the potential lipid-lowering effect of ACLY inhibition by **326E** and **326Z**, golden hamsters fed a high-fat and high-cholesterol (HFHC) diet for 2 weeks were used as a hyperlipidemia model (Fig. 1H). **326E** and **326Z** (10 mg/kg) were orally administered for 2 weeks, and BA (30 mg/kg) was used as a positive control. The average serum contents of TG, TC and LDL-C in vehicle-treated animals increased dramatically compared to the normal chow group, and these levels were significantly reduced after daily **326E** treatment compared to the vehicle group. The reduction effects after 10 mg/kg **326E** treatment were comparable to 30 mg/kg BA treatment (Fig. 1I–K). Although there was objective *de novo* lipogenesis inhibition in primary hepatocytes, **326Z** treatment reflected moderation of the lipid-lowering effects compared to **326E** and BA treatment (Fig. 1I–K). The effect on HDL-C after **326E** and **326Z** treatment was slight (Fig. 1L). Taken together, these results demonstrate that isomer **326E** but not **326Z** effectively reduces lipogenesis and improves dyslipidemia in a rodent model of HFHC diet-induced hyperlipidemia.

2.4. Identification of the CoA thioester of **326E** as a novel ACLY inhibitor

As previously reported, BA rapidly forms a CoA thioester (BA-CoA) through ACSVL1 in the liver, which directly inhibits

ACLY with $K_i = 2 \mu\text{mol/L}$. To gain further insights into ACLY inhibition, we synthesized BA-CoA and **326E**-CoA as shown in Scheme 3^{41,44}. Thioesters were prepared by activating BA or **326E** with 1,1'-carbonyldiimidazole in dry DCM, followed by reaction with the trilithium salt of CoA in an aqueous bicarbonate solution. The resulting product was purified using semi-preparative solid-phase extraction to afford thioesters BA-CoA or **326E**-CoA respectively.

To assess the effects of ACLY inhibition *in vitro*, we evaluated BA-CoA and **326E**-CoA for ACLY inhibition in a cell-free system using the ADP-Glo assay. In accordance with previous studies, BA-CoA incubation inhibited recombinant human ACLY activity with an $\text{IC}_{50} = 10.56 \pm 1.46 \mu\text{mol/L}$ (Fig. 2A). The **326E**-CoA molecule potently inhibited ACLY with an $\text{IC}_{50} = 5.31 \pm 1.21 \mu\text{mol/L}$ (Fig. 2B). Furthermore, kinetic analyses of **326E**-CoA against ACLY substrates were performed to investigate the mechanism of ACLY inhibition. **326E**-CoA was a competitive inhibitor of the CoA substrate with an inhibition constant $K_i = 2.51 \mu\text{mol/L}$. Meanwhile, **326E**-CoA exhibited noncompetitive inhibitor kinetics relative to citrate (Fig. 2C and D, Supporting Information Table S2). In addition, we determined that **326E**-CoA affects substantial ACLY stabilization using thermal shift assays (Supporting Information Fig. S1). These results demonstrate that the CoA-conjugated form of **326E** is a novel ACLY inhibitor, and that the **326E**-CoA-conjugated form competes for CoA binding at ACLY and inhibits catalytic activity.

BA is converted to BA-CoA in the liver by ACSVL1. Firstly, we analyzed the long-chain acyl-CoA synthetases (*Acs1*) family genes expression. Our results indicated that only *Acs11* was high expression (100 folds higher than *Acs11*) in the liver (Supporting Information Fig. S2). To investigate the potential mechanism of **326E**-CoA formation, we performed a series of studies and revealed that **326E** was coupled with CoA to form **326E**-CoA *in vitro* and *in vivo*. Fatty acids (monocarboxylic acids) with C14 to C24 carbon chain lengths, which are potential substrates of ACSLs, were competitive for **326E**-CoA formation in the microsomes (Supporting Information Fig. S3). Moreover, to further determine whether **326E**-CoA was transformed by **326E** treatment *in vivo*, a single dose of **326E** was orally administered to mice. The content of **326E**-CoA was measured using LC-MS/MS. Consistently, **326E**-CoA was detected in the liver ($2.11 \pm 0.84 \mu\text{g/g}$ liver) after 1 h of **326E** treatment, and the coupled rate of **326E** to **326E**-CoA was 11.89% (Supporting Information Table S3). These results indicate that **326E** is converted to **326E**-CoA in the liver by ACSLs-related enzymes.

Next, we used primary hepatocytes isolated from mice to further explore the inhibition of *de novo* lipogenesis. **326E** treatment inhibited fatty acids and cholesterol biosynthesis dose dependently when using [1,2-¹⁴C]-acetate and [¹⁴C]-citrate as precursors. The IC_{50} values of fatty acids and cholesterol synthesis inhibition were 0.76 ± 0.20 and $1.82 \pm 1.89 \mu\text{mol/L}$ respectively for [1,2-¹⁴C]-acetate incorporation (Fig. 2E). Meanwhile, **326E** treatment inhibited fatty acids and cholesterol biosynthesis with IC_{50} values of 13.26 ± 1.89 and $5.53 \pm 2.49 \mu\text{mol/L}$, respectively after [¹⁴C]-citrate incorporation (Fig. 2F). Besides, **326E**

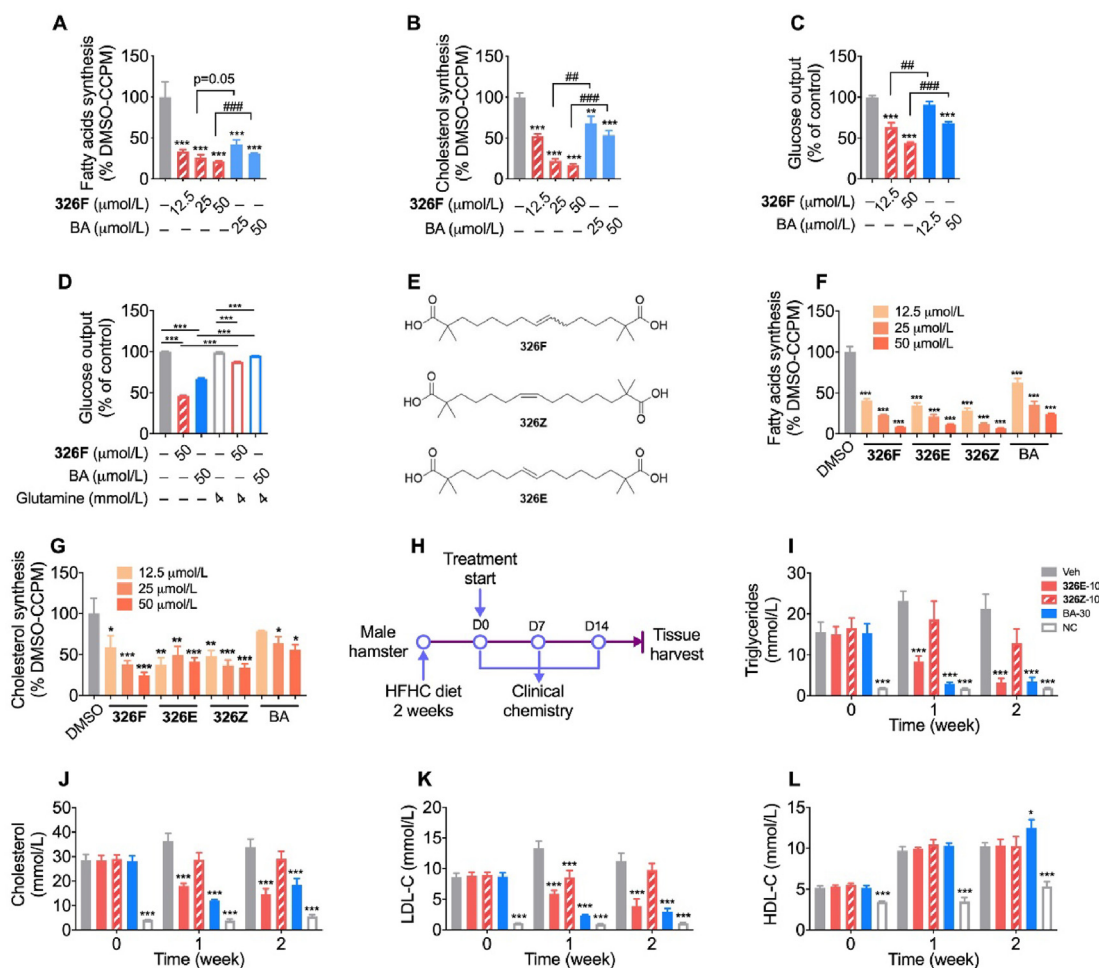
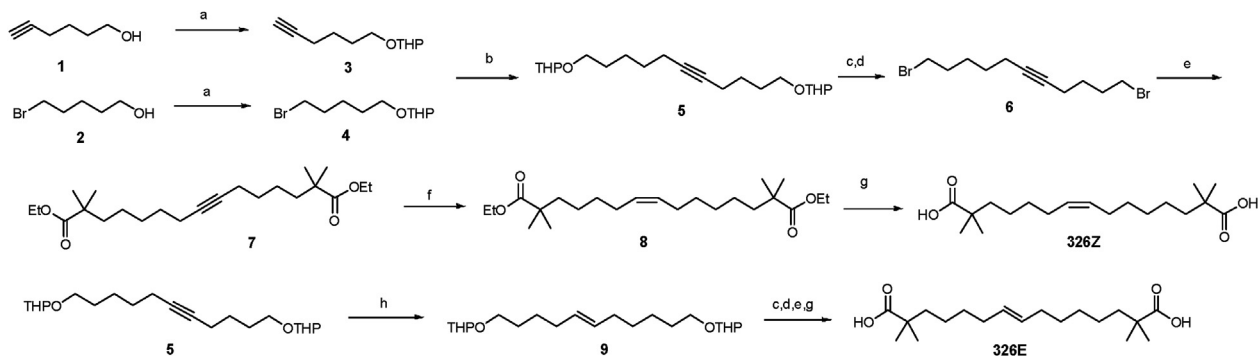


Figure 1 Identification of **326E** inhibits lipogenesis and gluconeogenesis in primary hepatocytes with more effective than BA. (A)–(B) Primary mouse hepatocytes were treated with the indicated concentration of **326F** or BA for 24 h. $0.1 \mu\text{Ci/well}$ [$1,2\text{-}^{14}\text{C}$]-acetate was added into the culture medium at last 4 h of incubation. The contents of [$1,2\text{-}^{14}\text{C}$]-acetate incorporated into fatty acids (A) and cholesterol (B) were measured. The radioactive content of lipids was normalized to DMSO group ($n = 4$); (C) Primary mouse hepatocytes were treated with the indicated concentration of **326F** or BA for 6 h. The rate of gluconeogenesis in the medium induced by pyruvate (2 mmol/L) and lactate (20 mmol/L) was measured. The content of glucose output was normalized to DMSO group ($n = 4$); (D) Primary mouse hepatocytes were treated with the indicated concentration of **326F** or BA for 6 h in the gluconeogenesis medium as (C), with or without supplied with 4.0 mmol/L L-glutamine in the indicated group. The content of glucose output was normalized to DMSO group ($n = 4$); (E) The structure of **326F**, **326Z** and **326E**; (F)–(G) Primary mouse hepatocytes contain $0.1 \mu\text{Ci/well}$ [$1,2\text{-}^{14}\text{C}$]-acetate were treated for 4 h with the indicated concentration of **326F**, **326E**, **326Z** and BA. The contents of [$1,2\text{-}^{14}\text{C}$]-acetate incorporated into fatty acids (F) and cholesterol (G) were measured. The radioactive content of lipids was normalized to DMSO group ($n = 3\text{--}4$); (H) The Schematic diagram of the experiment. Male golden hamsters fed an HFHC diet for 2 weeks, then oral administration of **326E** (10 mg/kg), **326Z** (10 mg/kg) and BA (30 mg/kg) for another 2 weeks ($n = 8$). HFHC diet, high fat high cholesterol diet (normal chow supplemented with 0.5% cholesterol, 23% fat and 5% Fructose, w/w); (I)–(L) Serum levels of TG (I), TC (J), LDL-C (K) and HDL-C (L) in the groups were determined and plotted at indicated time. The hamsters were fasted overnight before the experiment. Data are mean \pm SEM; * $P < 0.05$, ** $P < 0.01$, *** $P < 0.001$ compared to DMSO or Veh. # $P < 0.05$, ## $P < 0.01$, ### $P < 0.001$ compared to indicated group. ns, not significant.

treatment reduced fatty acids and cholesterol biosynthesis when traced by $^3\text{H}\text{-H}_2\text{O}$ and $^{14}\text{C}\text{-glucose}$ (Fig. 2G–J). **326E** was coupled to **326E**-CoA by ACSLs-related enzymes. Furthermore, we utilized triacsin C, an inhibitor of ACSLs family enzymes, including ACSVL1, to confirm the requirement for CoA thioester conjugation. **326E** treatment reduced lipogenesis in a dose dependent manner. However, pretreatment with triacsin C for 30 min attenuated *de novo* lipogenesis inhibition by **326E** (Fig. 2K and L). **326E** treatment displayed a negligible inhibitory effect on *de novo* lipogenesis inhibition in the human hepatoma cell line

HepG2, due to the slight ACSVL1 expression as reported (Fig. 2M and N, Supporting Information Fig. S4). These results indicate that the reduction of *de novo* lipogenesis by **326E** is dependent on CoA thioester transformation.

Moreover, to specifically investigate the role of ACLY in **326E**-attenuated lipogenesis, hepatocytes isolated from ACLY KO mice (*Acly* *ff:cre*) and wild-type mice (*Acly* *ff*) were utilized (Supporting Information Fig. S5). We observed reduced fatty acids and cholesterol biosynthesis as a result of **326E** treatment in hepatocytes from *Acly* *ff* but these results were attenuated in *Acly* *ff*



Scheme 2 Synthesis of **326E** and **326Z**. Condition: a) PPTS, DHP, DCM. b) *n*-BuLi, HMPA, THF. c) TsOH, MeOH. d) CBr₄, PPh₃, DCM. e) ethyl isobutyrate, LDA, THF. f) H₂, Ni(OAc)₂, NaBH₄, ethylene diamine, EtOH. g) KOH, EtOH, H₂O. h) LiAlH₄, Ethylene glycol diethyl ether.

f. cre hepatocytes, suggesting that ACLY inhibition was required for **326E**-facilitated lipogenesis inhibition (Fig. 2O and P). Together, these data suggest that treatment with the small molecule **326E** ameliorates lipogenesis in the hepatocytes through ACLY inhibition.

2.5. The *in vivo* pharmacokinetics of **326E**

To increase the solubility and *in vivo* exposure of **326E** based on the weak acid form, we screened the salt types, and sodium salt was selected for further development due to its good solubility and stability. The *in vivo* pharmacokinetics of **326E** were examined in mice and dogs after intravenous (iv) and oral (*po*) administration (Table 1). Following iv administration, **326E** demonstrated low plasma steady-state clearance (CL) in mice (1.31 mL/min/kg) and in dogs (0.13 mL/min/kg). The steady state distribution volumes (*V*_{ss}) were 0.33 L/kg in mice and 0.29 L/kg in dogs.

Following oral administration at the indicated dose (10 mg/kg in mice and 5 mg/kg in dogs), **326E** was rapidly absorbed (Supporting Information Tables S4 and S5). The mean terminal half-life (*t*_{1/2}) value of **326E** was 3.79 h in mice and 27.40 h in dogs (Table 1). These results indicated that **326E** is orally bioavailable and has appropriate pharmacokinetic properties for use in mice and dogs.

2.6. Oral administration of **326E** reduces hepatic lipogenesis and VLDL-TG secretion

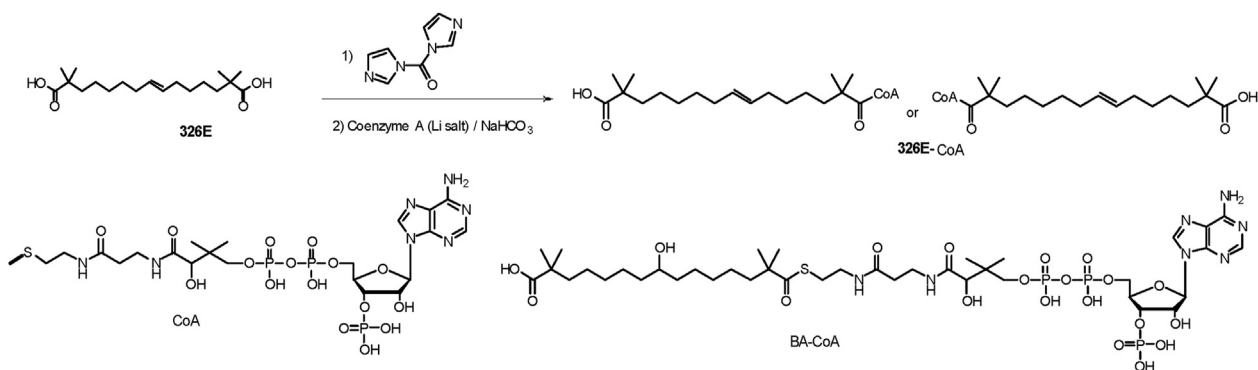
To evaluate its impact on lipogenesis *in vivo*, we examined the hepatic *de novo* lipogenesis inhibitory effect of **326E** (Fig. 3A). Oral administration of **326E** reduced the incorporation of [1,2-¹⁴C]-acetate into hepatic fatty acids and cholesterol in a dose

dependent manner (Fig. 3B and C). Since **326E** was coupled to the active agent **326E**-CoA in the liver by ACSLs, we further investigated the effect of lipogenesis after **326E** treatment in other tissues. Consistently, our data showed that **326E** treatment reduced lipogenesis specifically in the liver but not obviously so in the muscle, heart, ileum, abdominal adipose or kidney tissues (Fig. 3D and E).

The development of hypercholesterolemia is generally due to an imbalance between lipid secretion and elimination. Hepatic VLDL-TG secretion into the circulation is an important mechanism of lipid output from the liver. To determine whether hepatic DNL inhibition by **326E** treatment prompted an acute lipid-lowering effect, hepatic VLDL-TG secretion was measured after oral administration of **326E** in a fasted-refed mouse model. We discovered that **326E** and BA treatment rapidly diminished the increase in plasma TG levels (Fig. 3F and G) and cholesterol levels (Fig. 3H and I) at the indicated times after intraperitoneal injection of the lipoprotein lipase (LPL) inhibitor tyloxapol (Fig. 3F and H). The TG and cholesterol AUC_{0-4 h} were decreased by 75.8% and 58.9% in response to 100 mg/kg **326E** treatment respectively (Fig. 3G and I). Consistent with the *in vitro* effect, these results indicated that oral administration of **326E** inhibits hepatic *de novo* lipogenesis and reduces VLDL-TG secretion *in vivo*.

2.7. Inhibition of ACLY by **326E** and BA increases cholesterol efflux *in vitro* and *in vivo*

According to previous studies, hepatic cholesterol efflux is mediated by ACLY^{30,31}. Inhibition of ACLY is relevant to the expression of the cholesterol efflux genes *Abcg5/8*. To estimate



Scheme 3 Synthesis of the CoA thioester of **326E** and BA.

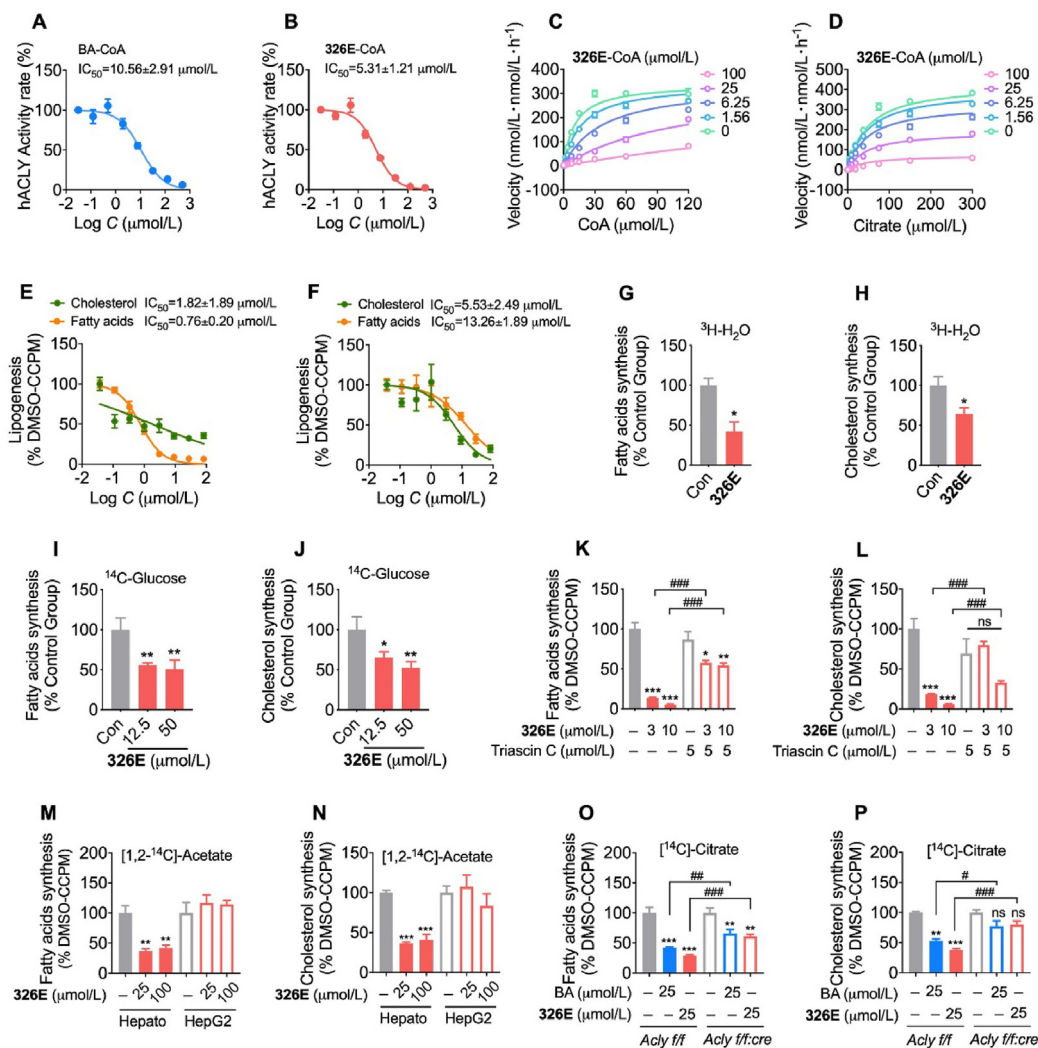


Figure 2 326E inhibits ACLY activity and suppresses lipid synthesis in primary hepatocytes isolated from mice. (A)–(B) Dose-dependent inhibition of purified, recombinant ACLY after incubated with BA-CoA (A) and 326E-CoA (B), the activity at control was defined as 100%; (C)–(D) Recombinant human ACLY was incubated with indicated concentrations of 326E-CoA coenzyme A (C) or citrate (D). K_i was calculated by Michaelis-Menten kinetic analysis; (E)–(F) Hepatocytes from mouse were exposed to DMEM with control or multiple doses of 326E for 4 h in the presence of [1,2- ^{14}C]-acetate (E) or [^{14}C]-citrate (F) as noted, and IC_{50} for *de novo* lipogenesis in the hepatocytes were generated; (G)–(J) Hepatocytes from mouse were exposed to DMEM with control or 326E for 4 h in the presence of [^3H]- H_2O or [^{14}C]-glucose as noted, fatty acids (G, I) and cholesterol (H, J) biogenesis in the hepatocytes were showed; (K)–(L) ACSLs inhibitor triacin C attenuates 326E induced lipogenesis in fatty acids (K) and cholesterol synthesis (L). Triacin C (5 $\mu\text{mol/L}$) was pre-treated for 30 min before 326E treatment; (M)–(N) Hepatocytes isolated from mice or HepG2 cell lines were exposed to DMEM with control or 326E for 4 h in the presence of [1,2- ^{14}C]-acetate as noted, and the radioactive contents of ^{14}C -fatty acids (M) and ^{14}C -cholesterol (N) incorporated by [1,2- ^{14}C]-acetate were counted by liquid scintillation counter; (O)–(P) Hepatocytes isolated from *Acly f/f* mice or *Acly f/f:cre* mice were exposed to DMEM with control, 326E or BA for 4 h in the presence of 0.1 $\mu\text{Ci/well}$ [^{14}C]-citrate as noted, and the radioactive contents of ^{14}C -fatty acids (O) and ^{14}C -cholesterol (P) incorporated by [^{14}C]-citrate were counted by liquid scintillation counter. Data are mean \pm SEM; * $P < 0.05$, ** $P < 0.01$, *** $P < 0.001$ compared to Control (Con). # $P < 0.05$, ## $P < 0.01$, ### $P < 0.001$ compared to indicated group. ns, not significant.

the cholesterol efflux efficacy of ACLY inhibition by 326E, we investigated the effect of the cholesterol efflux rate after 326E treatment *in vitro* and *in vivo*. Primary hepatocytes were co-incubated with 15 $\mu\text{g/mL}$ cholesterol (in 420 $\mu\text{g/mL}$ M- β -CD) and BA or 326E for 24 h, and *Abcg5/8* mRNA and intracellular cholesterol were measured. Expression of the cholesterol efflux-related genes *Abcg5* and *Abcg8* was upregulated dose-dependently in response to 326E treatment (Fig. 4A). Consistently, 326E or BA treatment significantly ameliorated

intracellular cholesterol accumulation (Fig. 4B). Next, we evaluated the effect of ACLY inhibitors on cholesterol efflux in hepatocytes as assessed by ^3H -labelled cholesterol according to the scheme shown in Fig. 4C. 326E or BA treatment markedly promoted cholesterol efflux into the cell culture medium, and the cholesterol efflux rate was much higher than that of the control group (Fig. 4D).

Hepatic cholesterol efflux occurs through ABCG5/8 transporters into the gallbladder and is then excreted into the intestine

Table 1 Preclinical pharmacokinetics of **326E** in mice and dogs.

| Species | Route | Dose (mg/kg) | CL (mL/min/kg) | V _{ss} (L/kg) | t _{1/2} (h) | T _{max} (h) | C _{max} (μg/mL) | AUC _{0-t} (μg·h/mL) |
|------------|-------|--------------|----------------|------------------------|----------------------|----------------------|--------------------------|------------------------------|
| ICR mice | iv | 10 | 1.31 | 0.33 | 4.55 | NA | NA | 138.00 |
| | po | 10 | NA | NA | 3.79 | 0.13 | 25.65 | 128.40 |
| Beagle dog | iv | 5 | 0.13 | 0.29 | 26.20 | NA | NA | 534.00 |
| | po | 5 | NA | NA | 27.40 | 0.25 | 39.60 | 419.00 |

Pharmacokinetic parameters were calculated from plasma concentration-time data and were reported as mean value (*n* = 6, sex in half). Solution formulation for iv pharmacokinetics were conducted using ddH₂O. Oral pharmacokinetics were conducted using 0.9% NaCl. NA = not applicable.

along with bile acids⁴⁵. To investigate the cholesterol efflux effect of **326E** *in vivo*, high cholesterol diet-induced mice (HCD mice) were orally administered a single dose of **326E** or BA for 24 h. Treatment with ACLY inhibitor **326E** or BA increased hepatic *Abcg5* and *Abcg8* mRNA expression (Fig. 4E). Meanwhile, cholesterol content in the gallbladder was much higher than that in the vehicle group, indicated a higher cholesterol efflux rate (Fig. 4F). We next evaluated the cholesterol efflux in HCD mice using ³H-labelled cholesterol after BA and **326E** treatment for 7 days (Fig. 4G). The fecal and hepatic radiolabeled cholesterol as well as bile acids were determined. ACLY inhibitor treatment

increased radiolabeled cholesterol but not bile acids excretion in feces (Fig. 4H and I). Consistent with this finding, much lower radiant quantities of radiolabeled cholesterol in the liver were observed (Fig. 4J). The radiolabeled ³H-bile acids were reduced in **326E**-treated mice compared to vehicle-treated mice, likely due to lower content of hepatic ³H-labeled cholesterol, which was as the result of higher ³H-cholesterol efflux after **326E** treatment (Fig. 4K). Similarly, we also observed that **326E** and BA treatment for 7 days significantly reduced hepatic cholesterol content in HCD mice (Fig. 4M and L). These findings suggest that the ACLY inhibitor increased cholesterol efflux in HCD mice and reduced

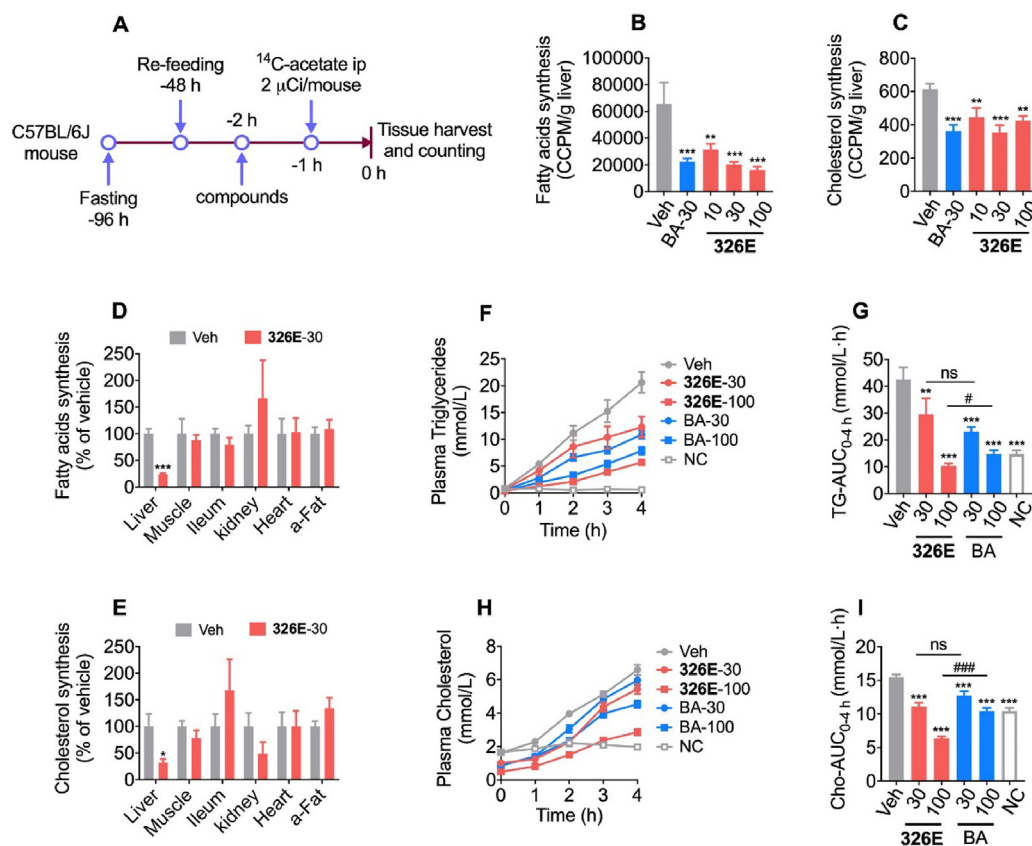


Figure 3 **326E** treatment reduces hepatic *de novo* lipogenesis and VLDL-TGs secretion. (A) Schematic diagram of **326E** treatment for hepatic *de novo* lipogenesis. Briefly, male C57BL/6J mice were fasted for 48 h followed by refeeding for another 48h. Animals then received **326E** treatment at multi-dose followed by an intraperitoneally injection with 2 μCi [1,2-¹⁴C] acetate (in B, C) and 5 μCi [1,2-¹⁴C] acetate (in D, E) 1 h later dosing. One hour after [1,2-¹⁴C] acetate injection, the mice were sacrificed after anesthetization, and the hepatic lipogenesis was calculated; (B)–(C) The rate of ¹⁴C-labeled hepatic *de novo* lipogenesis after **326E** (10, 30, 100 mg/kg) and BA (30 mg/kg) treatment (*n* = 5–6); (D)–(E) The rate of ¹⁴C-labeled *de novo* lipogenesis after **326E** (30 mg/kg) in the liver, leg muscle, ileum, kidney, heart and abdominal fat (a-Fat) (*n* = 7–8); (F)–(I) Plasma TG (F) and TC (H) concentration under tyloxapol (600 mg/kg) injection were measured after **326E** and BA treatment at the indicated dose (*n* = 10). The area under the curve of TG level (G) and TC (I) in 4 h of VLDL-TGs secretion were shown. Data are mean ± SEM; **P* < 0.05, ***P* < 0.01, ****P* < 0.001 compared to Veh. #*P* < 0.05, ###*P* < 0.01, ####*P* < 0.001 compared to indicated group. ns, not significant.

hepatic cholesterol content, which at least partly contributed to the lipid-lowering effect *in vivo*.

2.8. 326E treatment improves hyperlipidemia in rodents and rhesus monkeys

To examine the potential clinical translation of our novel ACLY inhibitor, we administered multiple doses of 326E therapy for 14 days to treat hyperlipidemia in an HFHC diet-induced hamster model (Fig. 5A). Compared to the vehicle group, body weight was

significantly decreased during the 2 weeks of 326E treatment at 15 mg/kg and 30 mg/kg, as well as BA treatment (Fig. 5B). In accordance with the reduced body weight, hamsters orally administered 326E exhibited a dose-dependent improvement in the hypolipidemic effect. 326E treatment (30 mg/kg) resulted in a 57.8% reduction in serum TC, 92.9% reduction in serum TG, and 72.8% reduction in serum LDL-C, confirming the hypolipidemic effect of 326E *in vivo* (Fig. 5C–E). Oral administration of 326E and BA also reduced serum HDL-C levels, likely due to the reduced serum LDL-C concentration (Fig. 5F).

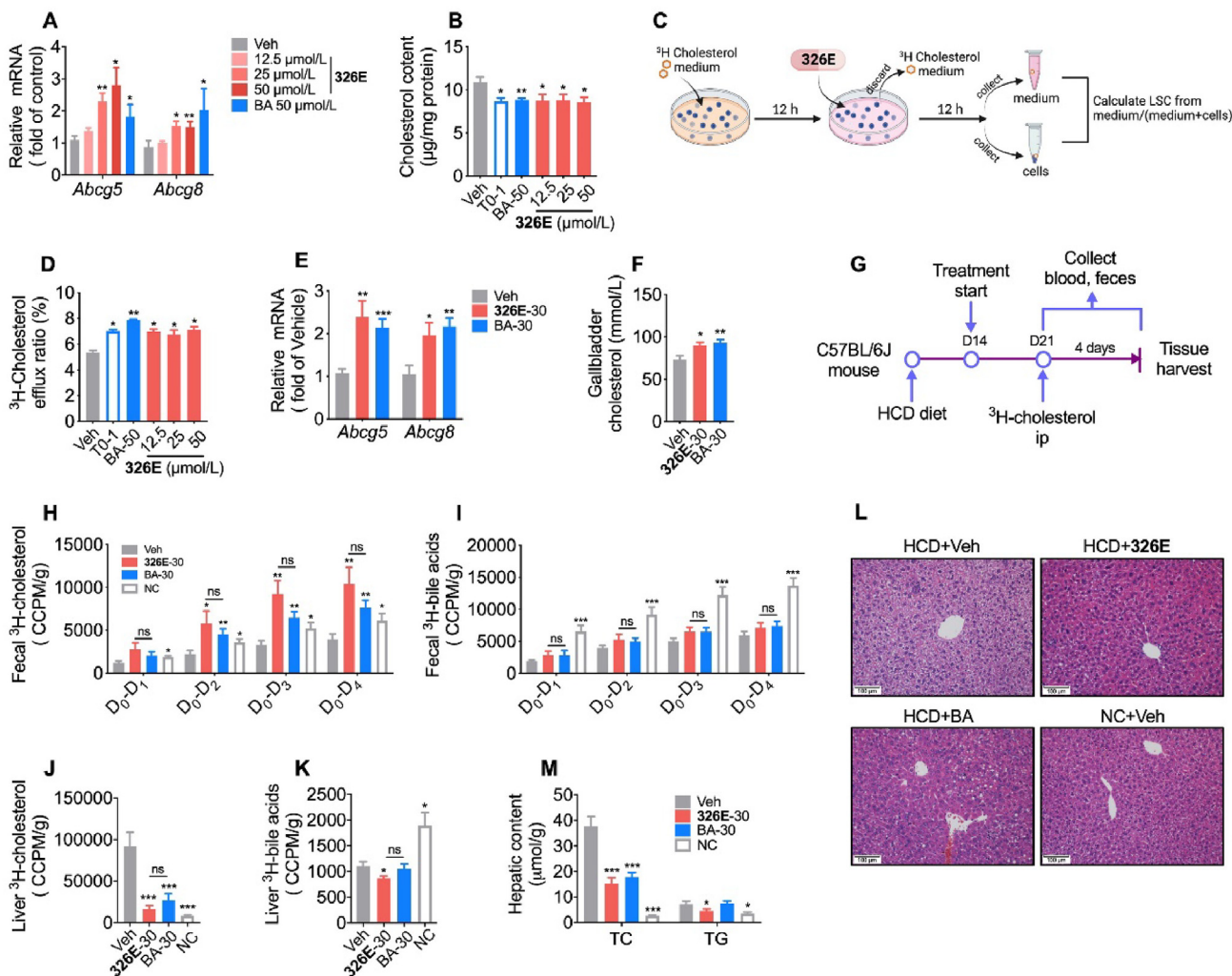


Figure 4 Treatment of ACLY inhibitors increase cholesterol efflux and reduce hepatic cholesterol in HCD mice. (A)–(B) The mRNA levels of *Abcg5* and *Abcg8* (A) and intracellular cholesterol (B) were detected in the primary mouse hepatocytes after 326E and BA (50 $\mu\text{mol/L}$) treatment for 24 h. During the incubation, 15 $\mu\text{g/mL}$ cholesterol (containing 420 $\mu\text{g/mL}$ M- β -CD) was added. The LXR agonist T0901317 (T0, 1 $\mu\text{mol/L}$) were used as positive control in (B); (C) The schematic diagram of cholesterol efflux in the primary hepatocytes was shown; (D) The cholesterol efflux rate was detected after 326E and BA (50 $\mu\text{mol/L}$) treatment for 12 h in primary hepatocytes. The LXR agonist T0901317 (1 $\mu\text{mol/L}$) were used as positive control; (E) Hepatic mRNA of *Abcg5* and *Abcg8* were measured after a single dose of 326E and BA 30 mg/kg for 24 h in HCD mice ($n = 5-6$); (F) The content of cholesterol in the gallbladder was detected after a single dose of 326E and BA 30 mg/kg for 24 h in HCD mice ($n = 5-6$); (G)–(K) ^3H -cholesterol and ^3H -bile acids content in the feces (H, I) and liver (J, K) were counted with scintillation liquid. Briefly, HCD mice were oral of 326E or BA for 7 days. On the 7th day of treatment, mice were received an intravenous tail vein injection of 2.5 μCi ^3H -cholesterol, which was dissolved in 100 μL intralipid (20%). Fecal samples were collected at indicated time after ^3H -cholesterol injection. Livers were harvested 24 h later at last dosing (G). The radioactive cholesterol (H, J) and ^3H -bile acids (I, K) were detected ($n = 5-6$); (L)–(M) The HCD mice were oral given with 326E and BA for 7 days. The livers were harvested after 4 h fasting. The representative pictures H&E staining (L) were shown. The contents of hepatic cholesterol (TC) and triglycerides (TG) were measured (M) ($n = 5-6$). Data are mean \pm SEM; * $P < 0.05$, ** $P < 0.01$, *** $P < 0.001$ compared to Veh. # $P < 0.05$, ## $P < 0.01$, ### $P < 0.001$ compared to indicated group. ns, not significant.

To predict the efficacy of **326E** in treating human hypercholesterolemia, rhesus monkeys with spontaneous hyperlipidemia were used to evaluate the lipid-lowering efficacy of **326E** (Fig. 6A). Atorvastatin at the clinically recommended dose (2.4 mg/kg) was used as a positive control (Fig. 6A, $n = 3$). Body weight was unchanged during treatment with **326E** or atorvastatin (Fig. 6B and C). In response to **326E** (20 mg/kg) treatment, plasma concentrations of TG and TC were reduced by 20.94% and 31.83%, respectively, compared to those at baseline (Fig. 6D–G). Plasma concentrations of LDL-C and ApoB100 were reduced by 20.11% and 20.88%, respectively, compared to those at baseline (Fig. 6H–K). During treatment, the efficacy of **326E** in lowering plasma TC, LDL-C and ApoB100 were comparable with atorvastatin, but TG content reduction after **326E** treatment was much effective (Fig. 6D and E). To evaluate the pharmacokinetics, we also examined the *in vivo* pharmacokinetics of **326E** in rhesus monkeys after the first dose administration. **326E** was rapidly absorbed ($T_{max} = 1.33 \pm 0.58$ h), and the mean terminal half-life ($t_{1/2}$) value was 49.47 ± 29.34 h in rhesus monkeys. The C_{max} of **326E** after oral administration was 139.22 ± 48.31 $\mu\text{g/mL}$ (Fig. 6L, Table 2). Accordingly, the $AUC_{0-24\text{ h}}$ of individual tendency was similar to the LDL-C lowering effect, suggesting a good relationship between *in vivo* exposure and lipid lowering efficacy (Fig. 6L and M).

Encouragingly, during the treatment period of **326E**, general organ function, as reflected by plasma creatine kinase (CK) for muscle injury and urea nitrogen for renal function, was similar before and after treatment (Supporting Information Fig. S6). Furthermore, AST and ALT levels in the plasma, which reflect liver function were decreased after **326E** treatment (Fig. 6N and O). Therefore, these results indicated that oral administration of **326E** might be an effective and safe therapy for hyperlipidemia treatment.

2.9. Inhibition of ACLY by 326E ameliorates atherosclerosis in ApoE^{-/-} mice

Excessive hepatic cholesterol biosynthesis contributes to the development of hypercholesterolemia and atherosclerosis. To assess the anti-atherosclerotic efficacy of chronic ACLY inhibition by

326E *in vivo*, we investigated the effect of **326E** in Western diet (WD)-induced ApoE^{-/-} mice. Once-daily oral administration of **326E** significantly decreased body weight gain during treatment with **326E** at 15, 30 and 60 mg/kg, but did not affect food intake (Supporting Information Figs. S7A and B). ACLY inhibition had a large impact on hepatic lipid levels. Accordingly, the contents of liver cholesterol and triglycerides were significantly decreased by **326E** treatment (Fig. 7A and B). Fasting content of cholesterol and LDL-C levels were lower than those of vehicle mice after 12 weeks of treatment with 30 mg/kg and 60 mg/kg **326E**, but not with 15 mg/kg or BA (30 mg/kg) treatment (Figs. S7C and D). To investigate the effect of **326E** on atherosclerosis, we stained the entire aortas of WD-induced ApoE^{-/-} mice with Sudan IV. The number and size of aortic plaques were significantly lower in **326E**-treated mice than in vehicle-treated mice and BA-treated mice (Fig. 7C and D), and a lower degree of atherosclerotic lesions was observed at the aortic valve in **326E**-treated mice as assessed by H&E staining (Fig. 7E and F). BA administration in clinical trials demonstrated a sustained reduction in the content of plasma high sensitivity Creactive protein (hsCRP) levels, so we next investigated the hsCRP lowering effect of **326E** treatment. In accordance with the reduced size of aortic plaques, the hsCRP content was reduced by more than 50% in response to multiple doses of **326E** (Fig. 7G). Expression of the inflammatory-related genes *Cd68*, *F4/80* and *Il-1 β* was also reduced in a dose dependent manner after **326E** treatment (Fig. 7H–J). In addition, gene expression of *Abcg5* and *Abcg8*, which are related to cholesterol efflux was induced after the long-term treatment with **326E**, indicating that the antiatherogenic effects of ACLY inhibition are also related to hepatic cholesterol efflux (Fig. 7K and L). Taken together, these results all indicate that treatment with the novel ACLY inhibitor **326E** improves atherosclerosis in WD-induced ApoE^{-/-} mice.

3. Discussion

Overnutrition is a driver of hepatic dysfunction and metabolic syndrome^{46,47}. Elevated hepatic *de novo* lipogenesis, attenuated clearance of circulating atherogenic LDL-C, and inflammatory

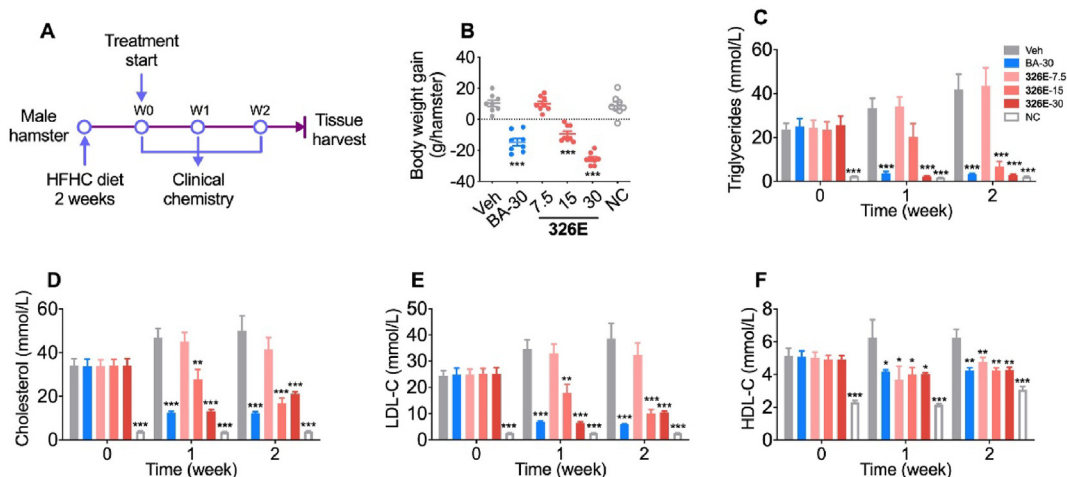


Figure 5 Effects of **326E** on lipid levels in blood of HFHC diet induced hyperlipidemia. (A) Schematic diagram of **326E** for hyperlipidemia treatment. Briefly, male golden hamsters were induced by HFHC diet for 2 weeks. Animals then received **326E** or BA treatment for another 2 weeks ($n = 8$). HFHC diet, high fat high cholesterol diet (normal chow supplemented with 0.5% cholesterol, 23% fat and 5% fructose, w/w); (B) Body weight gain were shown after **326E** treatment for 2 weeks; (C)–(F) Serum levels of TG (C), TC (D), LDL-C (E), and HDL-C (F) before and during the treatment period were shown. The oral dose of BA was 30 mg/kg. Data are mean \pm SEM; * $P < 0.05$, ** $P < 0.01$, *** $P < 0.001$ compared to Veh.

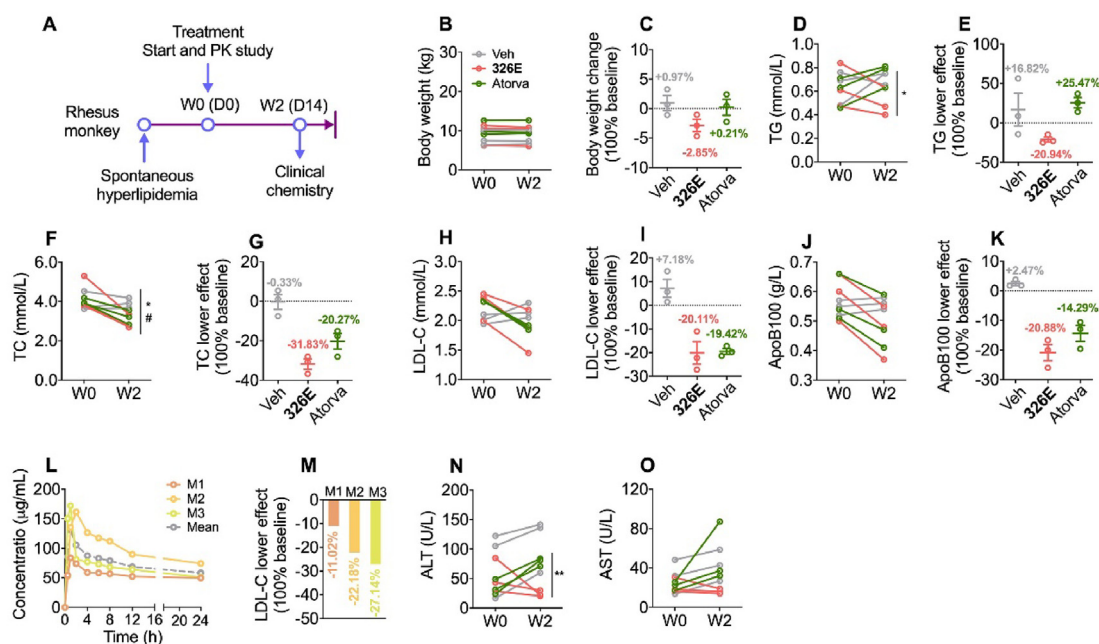


Figure 6 Lipid lowering efficacy and safety evaluation of **326E** in monkeys with hyperlipidemia. (A) Schematic diagram of **326E** treatment in rhesus monkey. Briefly, 6–20 years old male rhesus monkey with mild or moderate hyperlipidemia for more than 2 years (LDL-C:1.94–2.45 mmol/L) were selected, and oral treated with Veh, atorvastatin (atorva, 2.4 mg/kg/day) or **326E** (20 mg/kg/day). $n = 3$ monkey per group; (B)–(C) Body weight change after 2 weeks treatment; (D)–(K) Plasma levels of TG (D), TC (F), LDL-C (H), ApoB100 (J) in rhesus monkey before and after 2 weeks treatment; percentage lipid lowering effect were showed compared to baseline TG (E), TC (G), LDL-C (I), ApoB100 (K) were shown; (L)–(M) Pharmacokinetic curve in each monkey (M1, M2, M3) was shown after the first dose of **326E** at indicated time (L), and percentage of LDL-C lowering after **326E** treated for 2 weeks in each monkey (M); (N)–(O) Plasma levels of ALT (N) and AST (O) before and after **326E** or atorvastatin treatment. Data are mean \pm SEM; * $P < 0.05$, ** $P < 0.01$, *** $P < 0.001$, Veh compared to **326E**; # $P < 0.05$, ## $P < 0.01$, ### $P < 0.001$, Veh compared to atorva.

stimulation has proven difficult to correct CVDs using currently available agents⁴⁸. Approaches attempting to reduce hepatic lipogenesis and TG-VLDL secretion by targeting ACLY inhibition have been shown to be an attractive approach for combatting hyperlipidemia^{35,41}.

Herein, we identified **326E**, a novel ACLY inhibitor, was conjugated to form **326E**-CoA in the liver. **326E**-CoA inhibited human recombinant ACLY activity *in vitro* through competing the binding site of CoA. However, the detailed working molecular mechanism needs to be further explored. **326E** treatment significantly reduced fatty acids and cholesterol biosynthesis, as well as long chain fatty acids elongation partially dependent on ACLY. Oral administration of **326E** improved hyperlipidemia and ameliorated atherosclerosis in animal models. In particularly, oral administration of **326E** for 2 weeks in rhesus monkeys resulted in good tolerance and lipid-lowering effects. All these results suggest that the novel ACLY inhibitor **326E** is promising for clinical translation.

Cholesterol efflux through cholesterol channels or bile acids into the intestine are the major routes for cholesterol metabolism. Recent *in vitro* studies have shown that the transcriptional repressor Period 2 (PER2) possesses multiple binding sites within

the *Abcg5/8* locus. Once ACLY was inhibited by BMS303141, the occupation of PER2 at the *Abcg5/8* promoter was reduced, leading to a notable increase in *Abcg5/8* expression in primary hepatocytes³¹. Treatment with the ACLY inhibitor BA significantly increases hepatic *Abcg5/8* gene expression *in vivo*³⁰. Our studies indicated that ACLY inhibition by **326E** and BA treatment increases cholesterol efflux *in vitro* and *in vivo*, which was associated with improved *Abcg5/8* gene expression. Our observation demonstrated that ACLY inhibitor treatment augments hypercholesterolemia not only by inhibiting *de novo* lipogenesis, but also inducing hepatic cholesterol efflux.

Hepatic *de novo* lipogenesis reduced by ACLY inhibitor treatment provides a different therapy mechanism from statin therapy. Although having a similar IC_{50} for ACLY inhibition *in vitro*, we observed that oral administration of **326E** improves WD-induced atherosclerosis in ApoE^{-/-} mice after 24 weeks of treatment, which was much more effective than oral treatment with BA for the same treatment period. **326E** treatment reduced aortic plaques by 60%–86.7%, while BA was only reduced plaques by 33.4% after treatment. In addition, compared to vehicle mice, hepatic cholesterol content after **326E** treatment was reduced by 50%, which was much stronger than that of BA

Table 2 Pharmacokinetics of **326E** in rhesus monkey with hyperlipidemia.

| Dose (mg/kg) | $t_{1/2}$ (h) | T_{max} (h) | C_{max} (μ g/mL) | AUC_{0-t} (μ g·h/mL) | $AUC_{0-\infty}$ (μ g·h/mL) |
|--------------|-------------------|-----------------|-------------------------|-----------------------------|----------------------------------|
| 20 | 49.47 \pm 29.34 | 1.33 \pm 0.58 | 139.22 \pm 48.31 | 1777.75 \pm 529.58 | 5681.43 \pm 1430.25 |

Pharmacokinetic parameters were calculated from plasma concentration–time data related to Fig. 6L and were reported as mean \pm SD ($n = 3$, male).

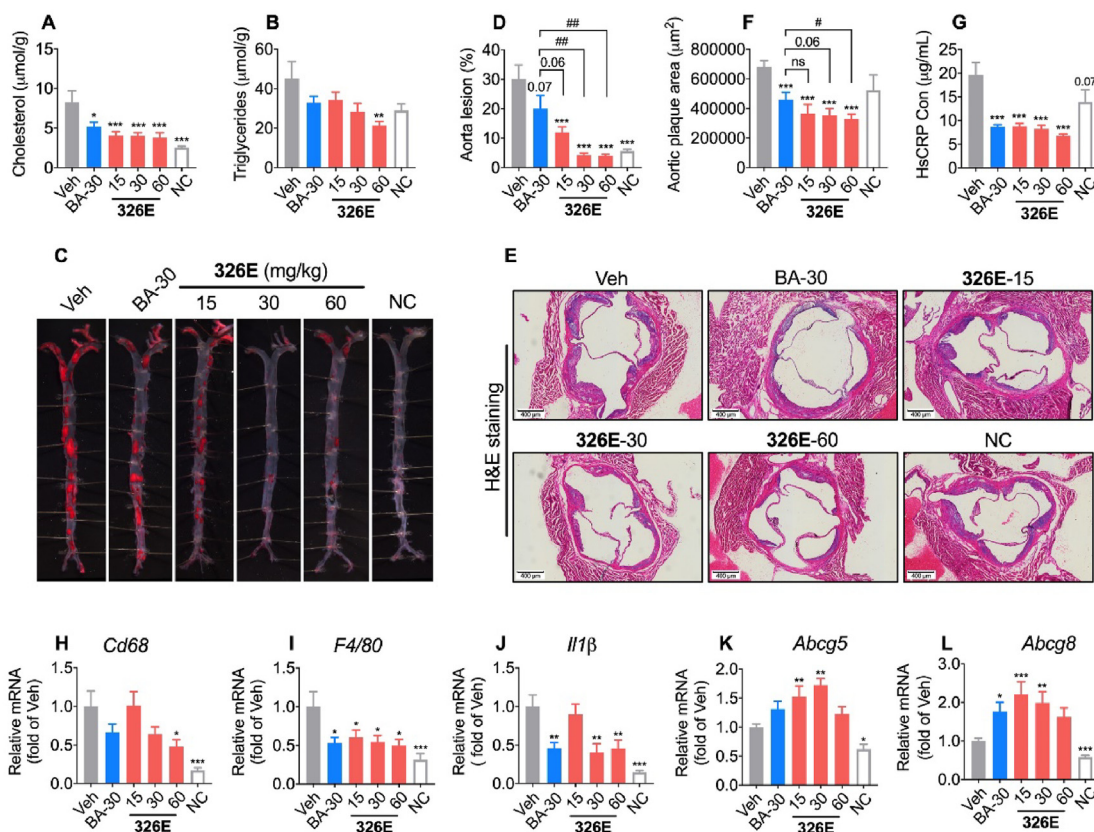


Figure 7 Treatment of **326E** decreases atherosclerosis in ApoE^{-/-} mice. (A)–(B) Male 6–8 weeks ApoE^{-/-} mice were induced by Western diet for 23–24 weeks. During the induction, mice were received **326E** or BA treatment once daily (*n* = 10). Western diet (normal chow supplemented with 0.2% cholesterol, *w/w*). Cholesterol levels (A) and triglycerides levels (B) in liver after 24 weeks treatment (*n* = 10); (C)–(D) Representative photographs of aortas from different groups after 24 weeks treatment (C); the quantifications (D) of the lesion areas in C (*n* = 10); (E)–(F) Representative H&E staining of cross-sections of aortic roots in different groups after 24 weeks treatment (E); the quantifications (F) of the lesion areas in E (*n* = 8–10); (G) Plasma contents of hsCRP in the indicated groups after 24 weeks treatment (*n* = 10); (H)–(L) Quantitative mRNA expression of *Cd68*, *F4/80*, *Il-1β*, *Abcg5*, *Abcg8* in the liver after **326E** and BA treatment. Data are mean ± SEM; **P* < 0.05, ***P* < 0.01, ****P* < 0.001 compared to Veh. #*P* < 0.05, ###*P* < 0.01, ####*P* < 0.001 compared to indicated group. ns, not significant.

treatment (37%). The observed dramatic pharmacological therapeutic effects after **326E** administration were likely due to the distinctive pharmacokinetic characteristics *in vivo*.

As in a previous study, the *in vitro* plasma protein-binding rate of BA was 95%–98% in mouse, rat, monkey and human plasma. Our unpublished data showed that **326E** exhibited a much higher plasma protein-binding rate in mice, dogs and humans (>99.8%). Higher blood exposure was detected after oral administration (*C*_{max}>100 μg/mL) of multiple dose's given. Although the free form of **326E** was approximately 0.5–1.5 μmol/L, which was close to the IC₅₀ of lipogenesis inhibition, the high plasma protein-binding rate and the tardy plasma steady-state clearance (1.31 mL/min/kg) resulted in continuous ACLY inhibition in the liver, which was closely related to the much greater reduction in hepatic cholesterol and plasma LDL-C. Our studies indicated that the plasma elimination half-life (*t*_{1/2}) among mice (3.79 h), dogs (27.4 h) and monkey (49.47 h) were extremely different. However, when we are considering the relationship between body size and physiologic function, which is known as allometry (*t*_{1/2} = 0.693 $\frac{K}{CL}$)⁴⁹, the *t*_{1/2} between mice and dogs are comparable (4.55 h in mice, and 21.5 h in dogs). However, in monkey study,

the animals are old rhesus monkey with hyperlipidemia (6–20 years old, and with moderate to mild hyperlipidemia for more than 2 years). The age and diseases state may decrease the clearance for drugs, that may be the reason why the *t*_{1/2} is longer (49.47 h) in monkey.

Previous studies have determined statins are strong inhibitors of mitochondrial complex III, which is associated with statin-induced myopathies¹⁰. In agreement with recent studies for BA^{41,43}, **326E** is a substrate of ACSLs (the specific synthetase of ACSLs isoform couples **326E** to **326E**-CoA needs to be further explored), which is coupled with CoA by ACSLs restricted in the liver. In fact, there was no significant inhibition of muscle *de novo* lipogenesis after **326E** administration in fasted-refed mouse model, and there was good tolerance in rhesus monkeys after **326E** treatment, indicating the tissue specificity of the **326E** response. Besides, the long term GLP toxicity study in beagle dogs indicated the no observed adverse effect level (NOAEL) was considered to 360 mg/kg (*C*_{max} = 569.50 μg/mL, AUC_{0–24 h} = 2472.50 μg·h/mL). Collectively, the high exposure and good tolerance property further supported that **326E** might be an effective and safe therapy for hypercholesterolemia.

4. Conclusions

In summary, our results show that pharmacological ACLY inhibition in the liver by **326E** leads to chronically sustainable improvements in lipid homeostasis, including lipid-lowering effects and the amelioration of atherosclerosis by reducing lipogenesis and hepatic cholesterol efflux. These findings demonstrate that **326E** has therapeutic potential and may serve as an oral agent for hypercholesterolemia. Recently, we have completed the IND application for this drug and have received approval for a clinical study for hypercholesterolemia (chictr.org.cn, ChiCTR2200057793), the first-in-human (FIH) results will be reported in due course.

5. Experimental

5.1. Chemistry

The experimental procedures and characterization of all compounds are provided in the Supporting Information.

5.2. Animal studies

For hepatocyte isolation and *de novo* lipogenesis *in vivo*, 8- to 12-week-old male C57BL/6J mice were purchased from Shanghai Model Organisms (Shanghai, China). Six- to eight-week-old male ApoE^{-/-} mice and six- to eight-week old male golden hamsters were purchased from Charles River (Beijing, China). ApoE^{-/-} mice were fed a high fat, high cholesterol diet (HFHC diet, D12079B, Research Diets, New Jersey, USA) for 23–24 weeks to induce atherosclerosis; hamsters were fed a high fat, high cholesterol, high fructose diet (C11953, Research Diets, New Jersey, USA) for 2–4 weeks to induce hyperlipidemia. C57BL/6J mice were fed a high cholesterol diet (HCD diet, D12109C, Research Diets, New Jersey, USA) for 2–4 weeks followed by analysis of cholesterol efflux. To obtain ACLY KO hepatocytes, ACLY-flox mice (*Aclyff* stock No: 43555, Jackson Laboratory, Bar Harbour, Maine, USA) were crossed with Albumin-Cre mice (stock No: 003574, Jackson Laboratory, Bar Harbor, Maine, USA) to generate liver-specific ACLY KO mice (*Aclyff:cre*). Rodents were housed in caging with 3–4 animals per cage and were maintained at 20–22 °C and at a humidity of 35 ± 5% under a 12 h light-dark cycle (7 AM on, 7 PM off). Food and water were available *ad libitum*. Age-matched animals were used for all experiments. All animals were sacrificed if needed under anaesthetic conditions, and animal welfare and animal experimental procedures were approved by the Animal Ethics Committee of the Shanghai Institute of Materia Medica, CAS, China.

5.3. *In vitro* ACLY assays

ACLY activity detection in the cell-free system was conducted as previously reported using an ADP-Glo dependent assay⁵⁰. Briefly, the reaction was performed in a 384-well plate, containing 2 µL substrate (5 µmol/L ATP, 30 µmol/L citrate, 15 µmol/L CoA) within kinase buffer (40 mmol/L Tris base, 10 mmol/L MgCl₂, 5 mmol/L DTT). The reaction was initiated by adding 20 nmol/L recombinant human ACLY protein and multiple doses of compounds into the well, followed by incubation for 30 min at 37 °C. In the reaction, ATPs were converted to ADPs by ACLY. The levels of ADPs in the well, representing the activity of ACLY,

were detected using the ADP-Glo kit (V9102, Promega, Madison, USA) according to the manufacturer's instructions. The enzymatic activity curve was analyzed using log (inhibitor) vs. normalized response-variable slope in GraphPad Prism.

5.4. Primary hepatocyte isolation

Primary hepatocytes were isolated from 8- to 12-week-old male C57BL/6J mouse⁵¹. Briefly, C57BL/6J mouse was anaesthetized and perfused with 20 mL calcium-free buffer from the inferior vena cava to the liver, and then the buffer containing collagenase I (LS004196, Worthington, USA) was added to breakdown the extracellular matrix and tight junctions at 37 °C. The liver was dissected in a sterile 6-cm cell culture dish containing 10 mL cold DMEM with 10% FBS, followed by filtration through a 70 µm cell strainer and centrifugation at 500 rpm for 3 min. Cells were then centrifuged with Percoll (P1644-100 ML, Sigma–Aldrich, USA) and living cells were resuspended in Hepato ZYME-SFM (17705-021, Thermo Fisher, USA) medium supplemented with 2 mmol/L L-glutamine, 20 units/mL penicillin and 20 µg/mL streptomycin. Then the hepatocytes were plated at 6 × 10⁵ cells/well in 6-well or 1.5 × 10⁵ cells/well in 24-well culture dishes precoated with 0.2% glue.

5.5. *In vitro* measurement of *de novo* lipogenesis

Hepatocytes were cultured in 6-well plates (6 × 10⁵ cells/well), and treated with compounds and [1,2-¹⁴C]-acetate, [¹⁴C]-citrate, [¹⁴C]-glucose, [³H]-H₂O (0.1 µCi/well) for the indicated times^{43,52}. The cells were washed with cold PBS and dissolved in 0.4–0.6 mL 0.5 mol/L KOH. Cholesterol and fatty acids were separated by saponification at 95 °C for 3 h with 0.4 mL KOH (20% methanol solution). The nonpolar cholesterol was extracted in 0.5 mL petroleum ether 3 times, and the polar fatty acids were extracted in 0.5 mL petroleum ether after adding 0.2 mL H₂O and 0.4 mL 5 mol/L H₂SO₄ for 3 times. The petroleum ether fractions were air-dried overnight at room temperature. Radioactive products were counted using a liquid scintillation counter.

5.6. *In vivo* measurement of *de novo* lipogenesis

The lipogenesis effect *in vivo* was assessed as previously described⁵². Briefly, male C57BL/6J mice weighing 20–25 g at 8–10 weeks of age were fasted for 48 h followed by refeeding for another 48 h. Next, animals received one dose of vehicle or experimental compounds. One hour after dosing, each mouse was intraperitoneally injected with the indicated dose of [1,2-¹⁴C]-acetate (NEC553001MC, PerkinElmer, USA). Mice were sacrificed 1 h after acetate injection and tissues were saponified. Isotope labelled fatty acids and cholesterol were then extracted and counted.

5.7. **326E**-CoA conjugated from **326E** *in vitro* and *in vivo*

In the *in vitro* study, mouse liver microsomes were obtained by ultracentrifugation according to a published previously protocol⁵³. The [¹⁴C]-**326E**-CoA conjugation rate was measured according to previously reported experimental methods⁴¹. [¹⁴C]-**326E**-CoA was separated from [¹⁴C]-**326E** by diethyl ether with two times of extractions. The contents of [¹⁴C]-**326E**-CoA in the aqueous phase were counted. In the *in vivo* study, the livers were harvested 1 h

after **326E** oral treatment, and the contents of **326E** and **326E**-CoA were measured separately using LC-MS/MS.

5.8. Plasma and liver lipid determination

Plasma total cholesterol (TC), triglycerides (TG), LDL-C and high-density lipoprotein cholesterol (HDL-C) levels were determined according to the manufacturer's instructions. To measure hepatic contents of triglycerides and cholesterol, liver tissues (30–40 mg) were homogenized in 0.5 mL cold PBS. A 0.4 mL homogenate was added to 1.4 mL of a mixture of $\text{CHCl}_3/\text{CH}_3\text{OH}$ (2:1, v/v), followed by shaking overnight at room temperature. The suspension was centrifuged at $2500\times g$ for 10 min, and the organic phase was transferred and air-dried. The residual organic substance was resuspended in 800 μL ethanol containing 1% Triton X-100, and the concentrations of triglycerides and cholesterol were determined using commercial kits.

5.9. VLDL-TG secretion experiment

Male C57BL/6J mice weighing 20–25 g at 8–10 weeks of age were fasted for 48 h followed by refeeding for another 48 h. Mice were divided into groups according to body weight during the refeeding period and treated with the indicated compounds for 3 days (one dose daily). Time 0-min blood samples were collected from tails after the last dose of compound treatment 30 min later, followed by intravenous injection of tyloxapol (600 mg/kg, dissolved in saline, T0307-10G, Sigma-Aldrich, USA). Blood samples were collected 1, 2, 3, 4 h after tyloxapol injection and were subjected to centrifugation at $12,000\times g$ for 2 min and stored at $-20\text{ }^\circ\text{C}$ until TG and cholesterol levels were assayed⁵⁴.

5.10. In vitro measurement of cholesterol efflux

First, 0.5 $\mu\text{Ci}/\text{mL}$ ^3H -cholesterol (NET139001MC, PerkinElmer, USA) and 15 $\mu\text{g}/\text{mL}$ cholesterol (in 420 $\mu\text{g}/\text{mL}$ M- β -CD) were added to the primary hepatocytes and cultured for 12 h ($37\text{ }^\circ\text{C}$, 5% CO_2). The medium containing ^3H -cholesterol, was then discarded, and the cells were gently washed 3 times with PBS. Cells were incubated in serum-free medium containing 15 $\mu\text{g}/\text{mL}$ cholesterol and **326E** (12.5, 25, 50 $\mu\text{mol}/\text{L}$), BA (50 $\mu\text{mol}/\text{L}$) or T0901317 (1 $\mu\text{mol}/\text{L}$) for another 12 h ($37\text{ }^\circ\text{C}$, 5% CO_2). Cell medium was carefully collected and centrifuged at $14,000\times g$ for 3 min to remove cellular debris, and 200 μL supernatant was transferred into a new microcentrifuge tube. The cells were washed 3 times with 200 μL PBS, and 200 μL 0.25 mol/L NaOH was added to lyse the cells. Transfer 150 μL of cell suspension to a new microcentrifuge tube. The ^3H -cholesterol content in the medium supernatant and cell suspension was counted in scintillation liquids (LSC). The cholesterol efflux ratio was determined as Eq. (1):

$$\text{Cholesterol efflux ratio (\%)} = \frac{^3\text{H-Cholesterol in the supernatant/}}{\text{(Supernatant } ^3\text{H-cholesterol} + \text{intracellular } ^3\text{H-cholesterol)}} \times 100 \quad (1)$$

The content of unlabeled intracellular cholesterol was measured using an AmplexTM Red Cholesterol Assay Kit (A12216, Thermo Fisher, MA, USA) according to the manufacturer's protocol.

5.11. In vivo measurement of cholesterol efflux

Male C57BL/6J mice weighing 20–25 g at 8–10 weeks of age were induced using a high cholesterol diet (HCD diet, D12109C, Research Diets, USA) for 2 weeks. Then, HCD mice were orally administered ETC-1002 (HY-12357, MedChemExpress, USA) or **326E** at 30 mg/kg for 7 days. On the 7th day of ACLY inhibitor treatment, mice were received an intravenous tail vein injection of 2.5 μCi ^3H -cholesterol, which was dissolved in 100 μL intralipid (20%). Fecal samples were collected 1, 2, 3, 4 days after ^3H -cholesterol injection. The feces samples were soaked and homogenized in ddH_2O ($w/v = 1:10$) overnight at $4\text{ }^\circ\text{C}$. Then, 100 μL homogenates were mixed with 400 μL KOH (20% in methanol), and saponified at $95\text{ }^\circ\text{C}$ for 3 h. The neutral cholesterol fraction was extracted 2 times using 800 μL petroleum ether. The extracts were dried overnight and counted in scintillation liquids. Feces were prepared by mixing with ddH_2O ($w/v = 1:10$) for 12 h at $4\text{ }^\circ\text{C}$. An equal volume of *tert*-butanol was added, and samples were extracted for 45 min at $37\text{ }^\circ\text{C}$. The supernatant, which contained bile acids, was transferred after centrifugation at $2000\times g$ for 15 min. The ^3H -bile acid content in the supernatants was measured in scintillation liquids⁵⁵.

5.12. Analysis of atherosclerotic lesions

To quantify the atherosclerotic area along the entire aorta, the aortic tree isolated from ApoE^{-/-} mice was dissected out and fixed in 70% ethanol for 10 min. Then, the lesions were stained with Sudan IV for 10 min, and rinsed twice with 70% ethanol (1.5 min/wash). The aortic tree was rinsed with PBS for 5 min to remove the residual ethanol, and the sudanophilic lesion area was assessed using Image J Pro Plus⁵⁶.

5.13. Histology

Tissue specimens were fixed in 4% paraformaldehyde (PFA), and paraffin-embedded sections were subjected to standard haematoxylin-eosin (H&E) staining.

5.14. Pharmacokinetic evaluation

ICR mice and beagle dogs were orally administered or intravenously injected with the indicated compounds, and serial blood samples were collected at the indicated times. Blood samples were centrifuged at 12,000 rpm for 2 min at $4\text{ }^\circ\text{C}$ to generate plasma. All plasma samples were kept frozen until analysis. The concentration of compounds in the plasma was detected using LC-MS/MS.

5.15. Rhesus monkey studies

Six to twenty-year old male rhesus monkeys with spontaneous mild or moderate hyperlipidemia for more than 2 years (LDL-C: 1.94–2.45 mmol/L) were selected, and then divided into three groups ($n = 3$). **326E** (20 mg/kg) or atorvastatin (2.4 mg/kg) was administered by oral gavage once daily for 2 weeks at Sichuan Primed Shines Bio-tech Co., Ltd., China. A comprehensive evaluation of clinical laboratory measurements was conducted, including TC, TG, LDL-C, ApoB100, ALT, AST, CK and BUN. After the first oral administration of **326E**, the PK study was performed.

5.16. Statistical analysis

All results are reported as the means \pm SEM. Differences between two groups were analyzed using a two-tailed unpaired Student's *t*-test. Differences in multiple groups were analyzed using one-way ANOVA (GraphPad Prism version 6.0 for Windows). Differences were considered significant when $P < 0.05$.

Acknowledgments

This work was supported by grants from the National Natural Science Foundation of China (92057116 and 82170872); the Medical Guidance Project of Shanghai Science and Technology Commission (20S11903400, China); the "Personalized Medicines-Molecular Signature-based Drug Discovery and Development" Strategic Priority Research Program of the Chinese Academy of Sciences (XDA12040328, China); the "State Key Laboratory of Drug Research" Shanghai Institute of Materia Medica, Chinese Academy of Sciences (SIMM2105KF-02, China); Natural Science Foundation of Shanghai's 2021 "Science and Technology Innovation Action Plan" (21ZR1475300, China); the Lingang Laboratory (LG-QS-202205-01, China).

Author contributions

Fajun Nan, Jingya Li, Zhifu Xie and Mei Zhang participated in the research design. Qian Song, Long Cheng, Xinwen Zhang, Gaolei Song, Yangming Zhang, Xinyu Sun, Min Gu, Chendong Zhou, Jianpeng Yin, Kexin Zhu and Xiaoyan Chen performed the experiments and data analysis. Zhifu Xie, Mei Zhang and Qian Song contributed to the preparation of this paper. Fajun Nan and Jingya Li contributed to discussion, review and editing the manuscript.

Conflicts of interest

Yangming Zhang received consultant allowance from Burgeon Therapeutics Co., Ltd. The other authors declare that the research was conducted in the absence of any commercial or financial relationships that could be construed as a potential conflict of interest.

Appendix A. Supporting information

Supporting data to this article can be found online at <https://doi.org/10.1016/j.apsb.2022.06.011>.

References

1. Ference BA, Ginsberg HN, Graham I, Ray KK, Packard CJ, Bruckert E, et al. Low-density lipoproteins cause atherosclerotic cardiovascular disease. 1. Evidence from genetic, epidemiologic, and clinical studies. A consensus statement from the European Atherosclerosis Society consensus panel. *Eur Heart J* 2017;**38**:2459–72.
2. Silverman MG, Ference BA, Im K, Wiviott SD, Giugliano RP, Grundy SM, et al. Association between lowering LDL-C and cardiovascular risk reduction among different therapeutic interventions: a systematic review and meta-analysis. *JAMA* 2016;**316**:1289–97.
3. Stone NJ, Robinson JG, Lichtenstein AH, Bairey Merz CN, Blum CB, Eckel RH, et al. 2013 ACC/AHA guideline on the treatment of blood cholesterol to reduce atherosclerotic cardiovascular risk in adults: a report of the American College of Cardiology/American Heart Association Task Force on Practice Guidelines. *Circulation* 2014;**129**:S1–45.
4. Karr S. Epidemiology and management of hyperlipidemia. *Am J Manag Care* 2017;**23**:S139–48.
5. Xiao C, Dash S, Morgantini C, Hegele RA, Lewis GF. Pharmacological targeting of the atherogenic dyslipidemia complex: the next frontier in CVD prevention beyond lowering LDL cholesterol. *Diabetes* 2016;**65**:1767–78.
6. Brautbar A, Ballantyne CM. Pharmacological strategies for lowering LDL cholesterol: statins and beyond. *Nat Rev Cardiol* 2011;**8**:253–65.
7. Uspst Force, Bibbins-Domingo K, Grossman DC, Curry SJ, Davidson KW, Epling Jr JW, et al. Statin use for the primary prevention of cardiovascular disease in adults: US preventive services task force recommendation statement. *JAMA* 2016;**316**:1997–2007.
8. Ford I, Murray H, McCowan C, Packard CJ. Long-term safety and efficacy of lowering low-density lipoprotein cholesterol with statin therapy: 20-year follow-up of West of Scotland Coronary Prevention Study. *Circulation* 2016;**133**:1073–80.
9. Istvan ES, Deisenhofer J. Structural mechanism for statin inhibition of HMG-CoA reductase. *Science* 2001;**292**:1160–4.
10. Schirris TJ, Renkema GH, Ritschel T, Voermans NC, Bilos A, van Engelen BG, et al. Statin-induced myopathy is associated with mitochondrial complex III inhibition. *Cell Metab* 2015;**22**:399–407.
11. Golomb BA, Evans MA. Statin adverse effects: a review of the literature and evidence for a mitochondrial mechanism. *Am J Cardiovasc Drugs* 2008;**8**:373–418.
12. Collins R, Reith C, Emberson J, Armitage J, Baigent C, Blackwell L, et al. Interpretation of the evidence for the efficacy and safety of statin therapy. *Lancet* 2016;**388**:2532–61.
13. Ashen MD, Foody JM. Evidence-based guidelines for cardiovascular risk reduction: the safety and efficacy of high-dose statin therapy. *J Cardiovasc Nurs* 2009;**24**:429–38.
14. Lagace TA. PCSK9 and LDL degradation: regulatory mechanisms in circulation and in cells. *Curr Opin Lipidol* 2014;**25**:387–93.
15. Cohen J, Pertsemlidis A, Kotowski IK, Graham R, Garcia CK, Hobbs HH. Low LDL cholesterol in individuals of African descent resulting from frequent nonsense mutations in PCSK9. *Nat Genet* 2005;**37**:161–5.
16. Stein EA, Mellis S, Yancopoulos GD, Stahl N, Logan D, Smith WB, et al. Effect of a monoclonal antibody to PCSK9 on LDL cholesterol. *N Engl J Med* 2012;**366**:1108–18.
17. Ray KK, Landmesser U, Leiter LA, Kallend D, Dufour R, Karakas M, et al. Inclisiran in patients at high cardiovascular risk with elevated LDL cholesterol. *N Engl J Med* 2017;**376**:1430–40.
18. Navarese EP, Kolodziejczak M, Schulze V, Gurbel PA, Tantry U, Lin Y, et al. Effects of proprotein convertase subtilisin/kexin type 9 antibodies in adults with hypercholesterolemia: a systematic review and meta-analysis. *Ann Intern Med* 2015;**163**:40–51.
19. Krahenbuhl S, Pavik-Mezzour I, von Eckardstein A. Unmet needs in LDL-C lowering: when statins won't do. *Drugs* 2016;**76**:1175–90.
20. Gotto Jr AM, Moon JE. Pharmacotherapies for lipid modification: beyond the statins. *Nat Rev Cardiol* 2013;**10**:560–70.
21. Sanders FW, Griffin JL. *De novo* lipogenesis in the liver in health and disease: more than just a shunting yard for glucose. *Biol Rev Camb Philos Soc* 2016;**91**:452–68.
22. Chiu S, Mulligan K, Schwarz JM. Dietary carbohydrates and fatty liver disease: *de novo* lipogenesis. *Curr Opin Clin Nutr Metab Care* 2018;**21**:277–82.
23. Hellerstein MK, Schwarz JM, Neese RA. Regulation of hepatic *de novo* lipogenesis in humans. *Annu Rev Nutr* 1996;**16**:523–57.
24. Srere PA. The citrate cleavage enzyme. I. Distribution and purification. *J Biol Chem* 1959;**234**:2544–7.
25. Tan M, Mosaoa R, Graham GT, Kasprzyk-Pawelec A, Gadre S, Parasido E, et al. Inhibition of the mitochondrial citrate carrier, SLC25A1, reverts steatosis, glucose intolerance, and inflammation in preclinical models of NAFLD/NASH. *Cell Death Differ* 2020;**27**:2143–57.
26. Kindt A, Liebisch G, Clavel T, Haller D, Hörmannspurger G, Yoon H, et al. The gut microbiota promotes hepatic fatty acid desaturation and elongation in mice. *Nat Commun* 2018;**9**:3760.

27. Martinez Calejman C, Trefely S, Entwisle SW, Luciano A, Jung SM, Hsiao W, et al. Mtorc2-AKT signaling to ATP-citrate lyase drives brown adipogenesis and *de novo* lipogenesis. *Nat Commun* 2020;**11**:575.
28. Guo L, Guo YY, Li BY, Peng WQ, Chang XX, Gao X, et al. Enhanced acetylation of ATP-citrate lyase promotes the progression of nonalcoholic fatty liver disease. *J Biol Chem* 2019;**294**:11805–16.
29. Lin R, Tao R, Gao X, Li T, Zhou X, Guan KL, et al. Acetylation stabilizes ATP-citrate lyase to promote lipid biosynthesis and tumor growth. *Mol Cell* 2013;**51**:506–18.
30. Samsouondar JP, Burke AC, Sutherland BG, Telford DE, Sawyez CG, Edwards JY, et al. Prevention of diet-induced metabolic dysregulation, inflammation, and atherosclerosis in LDLR^{-/-} mice by treatment with the ATP-citrate lyase inhibitor bempedoic acid. *Arterioscler Thromb Vasc Biol* 2017;**37**:647–56.
31. Molusky MM, Hsieh J, Lee SX, Ramakrishnan R, Tascou L, Haeusler RA, et al. Metformin and amp kinase activation increase expression of the sterol transporters ABCG5/8 (ATP-binding cassette transporter g5/g8) with potential antiatherogenic consequences. *Arterioscler Thromb Vasc Biol* 2018;**38**:1493–503.
32. Beigneux AP, Kosinski C, Gavino B, Horton JD, Skarnes WC, Young SG. ATP-citrate lyase deficiency in the mouse. *J Biol Chem* 2004;**279**:9557–64.
33. Wang Q, Jiang L, Wang J, Li S, Yu Y, You J, et al. Abrogation of hepatic ATP-citrate lyase protects against fatty liver and ameliorates hyperglycemia in leptin receptor-deficient mice. *Hepatology* 2009;**49**:1166–75.
34. Wang Q, Li S, Jiang L, Zhou Y, Li Z, Shao M, et al. Deficiency in hepatic ATP-citrate lyase affects VLDL-triglyceride mobilization and liver fatty acid composition in mice. *J Lipid Res* 2010;**51**:2516–26.
35. Pinkosky SL, Groot PHE, Lalwani ND, Steinberg GR. Targeting ATP-citrate lyase in hyperlipidemia and metabolic disorders. *Trends Mol Med* 2017;**23**:1047–63.
36. Ference BA, Ray KK, Catapano AL, Ference TB, Burgess S, Neff DR, et al. Mendelian randomization study of acly and cardiovascular disease. *N Engl J Med* 2019;**380**:1033–42.
37. Granchi C. Atp citrate lyase (acly) inhibitors: an anti-cancer strategy at the crossroads of glucose and lipid metabolism. *Eur J Med Chem* 2018;**157**:1276–91.
38. Feng X, Zhang L, Xu S, Shen AZ. ATP-citrate lyase (acly) in lipid metabolism and atherosclerosis: an updated review. *Prog Lipid Res* 2020;**77**:101006.
39. Ray KK, Bays HE, Catapano AL, Lalwani ND, Bloedon LT, Sterling LR, et al. Safety and efficacy of bempedoic acid to reduce LDL cholesterol. *N Engl J Med* 2019;**380**:1022–32.
40. Goldberg AC, Leiter LA, Stroes ESG, Baum SJ, Hanselman JC, Bloedon LT, et al. Effect of bempedoic acid vs placebo added to maximally tolerated statins on low-density lipoprotein cholesterol in patients at high risk for cardiovascular disease: the clear wisdom randomized clinical trial. *JAMA* 2019;**322**:1780–8.
41. Pinkosky SL, Newton RS, Day EA, Ford RJ, Lhotak S, Austin RC, et al. Liver-specific ATP-citrate lyase inhibition by bempedoic acid decreases LDL-C and attenuates atherosclerosis. *Nat Commun* 2016;**7**:13457.
42. Burke AC, Telford DE, Sutherland BG, Edwards JY, Sawyez CG, Barrett PHR, et al. Bempedoic acid lowers low-density lipoprotein cholesterol and attenuates atherosclerosis in low-density lipoprotein receptor-deficient (LDLR^{+/-} and LDLR^{-/-}) yucatan miniature pigs. *Arterioscler Thromb Vasc Biol* 2018;**38**:1178–90.
43. Pinkosky SL, Filippov S, Srivastava RA, Hanselman JC, Bradshaw CD, Hurley TR, et al. AMP-activated protein kinase and ATP-citrate lyase are two distinct molecular targets for ETC-1002, a novel small molecule regulator of lipid and carbohydrate metabolism. *J Lipid Res* 2013;**54**:134–51.
44. Pal M, Khanal M, Marko R, Thirumalairajan S, Bearne SL. Rational design and synthesis of substrate-product analogue inhibitors of α -methylacyl-coenzyme a racemase from mycobacterium tuberculosis. *Chem Commun (Camb)* 2016;**52**:2740–3.
45. Graf GA, Yu L, Li WP, Gerard R, Tuma PL, Cohen JC, et al. ABCG5 and ABCG8 are obligate heterodimers for protein trafficking and biliary cholesterol excretion. *J Biol Chem* 2003;**278**:48275–82.
46. Whaley-Connell A, Sowers JR. Indices of obesity and cardiometabolic risk. *Hypertension* 2011;**58**:991–3.
47. Farzadfar F, Finucane MM, Danaei G, Pelizzari PM, Cowan MJ, Paciorek CJ, et al. National, regional, and global trends in serum total cholesterol since 1980: systematic analysis of health examination surveys and epidemiological studies with 321 country-years and 3.0 million participants. *Lancet* 2011;**377**:578–86.
48. Michos ED, McEvoy JW, Blumenthal RS. Lipid management for the prevention of atherosclerotic cardiovascular disease. *N Engl J Med* 2019;**381**:1557–67.
49. Grover A, Benet LZ. *Clinical pharmacokinetics and pharmacodynamics. Encyclopedia of pharmaceutical science and technology*. 4th ed. CRC Press; 2013. p. 473–87.
50. Wei J, Leit S, Kuai J, Therrien E, Rafi S, Harwood Jr HJ, et al. An allosteric mechanism for potent inhibition of human ATP-citrate lyase. *Nature* 2019;**568**:566–70.
51. Li WC, Ralphs KL, Tosh D. Isolation and culture of adult mouse hepatocytes. *Methods Mol Biol* 2010;**633**:185–96.
52. Sun SM, Xie ZF, Zhang YM, Zhang XW, Zhou CD, Yin JP, et al. Ampk activator c24 inhibits hepatic lipogenesis and ameliorates dyslipidemia in HFHC diet-induced animal models. *Acta Pharmacol Sin* 2021;**42**:585–92.
53. Campbell RL, Supnick JD, Hettrick JM, Nigro ND. Rat liver microsome-mediated *N*-demethylation and mutagenicity of azoxy-methane. *Cancer Res* 1978;**38**:4585–90.
54. Lam TK, Gutierrez-Juarez R, Poci A, Bhanot S, Tso P, Schwartz GJ, et al. Brain glucose metabolism controls the hepatic secretion of triglyceride-rich lipoproteins. *Nat Med* 2007;**13**:171–80.
55. Xie Y, Kennedy S, Sidhu R, Luo J, Ory DS, Davidson NO. Liver x receptor agonist modulation of cholesterol efflux in mice with intestine-specific deletion of microsomal triglyceride transfer protein. *Arterioscler Thromb Vasc Biol* 2012;**32**:1624–31.
56. Tang JJ, Li JG, Qi W, Qiu WW, Li PS, Li BL, et al. Inhibition of srebp by a small molecule, betulin, improves hyperlipidemia and insulin resistance and reduces atherosclerotic plaques. *Cell Metab* 2011;**13**:44–56.